Effect of Li-deficiency impurities on the electron-overdoped LiFeAs superconductor

Meng Wang, Miaoyin Wang, Hu Miao, S. V. Carr, D. L. Abernathy, M. B. Stone, X. C. Wang, Lingyi Xing, C. Q. Jin, Xiaotian Zhang, Jiangping Hu, Tao Xiang, Hong Ding, and Pengcheng Dai

Phys. Rev. B **86**, 144511 — Published 11 October 2012

DOI: 10.1103/PhysRevB.86.144511

Effect of Li-deficiency impurities on the electron-overdoped LiFeAs superconductor

Meng Wang,[1] Miaoyin Wang,[2] Hu Miao,[1] S. V. Carr,[2] D. L. Abernathy,[3] M. B. Stone,[3] X. C. Wang,[1] Lingyi Xing,[1] C. Q. Jin,[1] Xiaotian Zhang,[1] Jiangping Hu,[1,4] Tao Xiang,[1] Hong Ding,[1] and Pengcheng Dai[2,1,*]

[1]*Beijing National Laboratory for Condensed Matter Physics, Institute of Physics, Chinese Academy of Sciences, Beijing 100190, China*
[2]*Department of Physics and Astronomy, The University of Tennessee, Knoxville, Tennessee 37996-1200, USA*
[3]*Quantum Condensed Matter Division, Oak Ridge National Laboratory, Oak Ridge, Tennessee 37831-6393, USA*
[4]*Department of Physics, Purdue University, West Lafayette, Indiana 47907, USA*

We use transport, inelastic neutron scattering, and angle resolved photoemission experiments to demonstrate that the stoichiometric LiFeAs is an intrinsically electron-overdoped superconductor similar to those of the electron-overdoped $NaFe_{1-x}T_xAs$ and $BaFe_{2-x}T_xAs_2$ (T = Co,Ni). Furthermore, we show that although transport properties of the stoichiometric superconducting LiFeAs and Li-deficient nonsuperconducting $Li_{1-x}FeAs$ are different, their electronic and magnetic properties are rather similar. Therefore, the nonsuperconducting $Li_{1-x}FeAs$ is also in the electron overdoped regime, where small Li deficiencies near the FeAs octahedra can dramatically suppress superconductivity through the impurity scattering effect.

PACS numbers: 74.25.Ha, 74.70.-b, 78.70.Nx

INTRODUCTION

Superconductivity in iron pnictides occurs near an antiferromagnetic (AF) instability [1, 2]. When the AF order in a nonsuperconducting (NSC) parent compound is suppressed by electron or hole doping, superconductivity emerges with the persistent short-range spin excitations directly coupled to the superconducting (SC) transition temperature T_c [3, 4]. While this general behavior is obeyed in most iron pnictide superconductors and suggests the importance of magnetism to the superconductivity of these materials [3–5], the only exception is the stoichiometric LiFeAs (Fig. 1a), which does not have a static AF ordered parent compound and superconducts with a relatively high T_c of ∼17 K without any doping [6–10]. Furthermore, a few percent of Li deficiencies in $Li_{1-x}FeAs$ can increase the resistivity and destroy superconductivity (Figs. 1b and 1c) [6, 11]. If antiferromagnetism is a common thread for the electron pairing and superconductivity in iron-based superconductors [12], one would expect that spin excitations in the SC and NSC $Li_{1-x}FeAs$ have some common features with other iron-based superconductors [3–5]. On the other hand, if antiferromagnetism is not important in iron-based superconductors, the mechanism of superconductivity in LiFeAs could in principle be different from other iron-based materials. Indeed, based on early angle resolved photoemission spectroscopy (ARPES) experiments, the absence of the static AF order in LiFeAs is believed to be caused by the poor nesting condition between the shallow hole-like Fermi pocket near the $\Gamma(0,0)$ point and the large electron Fermi surface at the $M(1,0)/(0,1)$ points in the Brillouin zone (Fig. 1d) [13]. These observations have fueled the suggestion that the mechanism of superconductivity in LiFeAs is due to a ferromagnetic instability and p-wave triplet pairing [13–15]. This is fundamentally different from all other iron pnictides, where the singlet electron pairing superconductivity and AF order are both believed to be associated with the sign reversed quasiparticle excitations between the hole and electron Fermi surfaces near the $\Gamma(0,0)$ and $M(1,0)/(0,1)$ points [16–19].

More recently, high-resolution ARPES experiments revealed the presence of nodeless SC gaps in the hole and electron Fermi pockes near the $\Gamma(0,0)$ and $M(1,0)/(0,1)$, respectively, in the SC LiFeAs, consistent with AF instead of ferromagnetic interactions [20]. Based on inelastic neutron scattering experiments on the SC single crystal LiFeAs, the low-energy spin excitations ($1.5 \leq E \leq 13$ meV) were found to respond to superconductivity and occur at the incommensurate wave vectors transverse to the in-plane AF electron-hole pocket nesting wave vector $Q_{AF} = (1,0)$ [21]. By noting that the electron-underdoped iron pnictide $BaFe_{2-x}T_xAs_2$ (T = Co,Ni) [22, 23] have transverse incommensurate static AF (spin-density-wave) order, the authors conclude that the SC LiFeAs should be compared with the electron-doped materials although its electron doping status is still unknown [21]. These results are different from the earlier neutron scattering experiments on powder SC LiFeAs [24] and single crystal NSC LiFeAs [25], where a large normal state spin gap (∼10 meV) has been reported. Given the rather confusing experimental situation, it is important to carry out new transport, neutron scattering, and ARPES experiments to sort out the differences in the electronic structures and spin excitations between the SC and NSC $Li_{1-x}FeAs$, and determine why $Li_{1-x}FeAs$ has no static AF order and why its superconductivity is so sensitive to a small amount of Li-deficiency [11].

Here we describe transport, inelastic neutron scattering, and ARPES experiments on the stoichiometric SC LiFeAs and Li-deficient NSC $Li_{1-x}FeAs$. We find

that a few percent Li-deficiency can completely suppress superconductivity and change transport properties but without significant effect on the sizes of the Fermi surfaces [20] and incommensurate spin excitations [21]. By comparing our results with previous work on the SC LiFeAs [20, 21], $NaFe_{1-x}Co_xAs$ [26–28], $BaFe_{2-x}T_xAs_2$ [29–31], and $LaFe_{1-y}Zn_yAsO_{1-x}F_x$ [32], we conclude that the stoichiometric LiFeAs is an intrinsically electron-overdoped superconductor similar to $NaFe_{1-x}Co_x$ with $x \approx 0.065$, and that Li deficiencies affect its SC properties similar to the Zn impurity effects in the electron-overdoped iron pnictide superconductors [32]. These results naturally explain the absence of the static AF order in $Li_{1-x}FeAs$, and why superconductivity in LiFeAs is so sensitive to the Li-deficiency. Therefore, the mechanism of superconductivity in LiFeAs is associated with AF spin excitations and not fundamentally different from all other iron-based superconductors [16–19].

RESULTS AND DISCUSSION

Our transport measurements on the SC and NSC $Li_{1-x}FeAs$ were carried out on a commercial physical properties measurement system using the four probe method. The inelastic neutron scattering experiments were performed on the ARCS time-of-flight chopper spectrometer at the spallation neutron source, Oak Ridge National laboratory [25]. The ARPES experiments were performed at the PGM beamline of the Synchrotron Radiation Center, Stoughton, Wisconson. The energy and angular resolutions of the ARPES measurements were set at ±20 meV and 0.2°, respectively. The samples were cleaved in situ and measured at 20 K in a vacuum better than 4×10^{-11} Torr. The incident photon energy was chosen to be $h\nu = 35$ eV. Our single crystals of the SC LiFeAs were grown using the self flux method with the ^{7}Li isotope to minimize neutron absorption. The method for growing the NSC $Li_{1-x}FeAs$ with natural Li was described previously [25]. The inductively coupled plasma analysis on the samples showed that the compositions of the NSC crystals are $Li_{0.94\pm0.01}FeAs$ [25]. Previous Rietveld analysis of the powder neutron diffraction data suggests that NSC $Li_{1-x}FeAs$ also have a small amount of As deficiency that we cannot determine from the inductively coupled plasma analysis [11]. To within the errors of our measurements, the SC LiFeAs was found to be stoichiometric. Figure 1b shows temperature dependence of the resistivity for the SC and NSC $Li_{1-x}FeAs$. Figure 1c plots the expanded view of the low-temperature resistivity for both samples, which reveals a $T_c = 16$ K for the SC LiFeAs and larger resistivity for the NSC $Li_{0.94}FeAs$. For inelastic neutron scattering measurements, we co-aligned approximately 3.95 grams of SC single crystals of LiFeAs with a mosaic of 2°. The NSC $Li_{0.94}FeAs$ was the same sample used in our previous measurements [25].

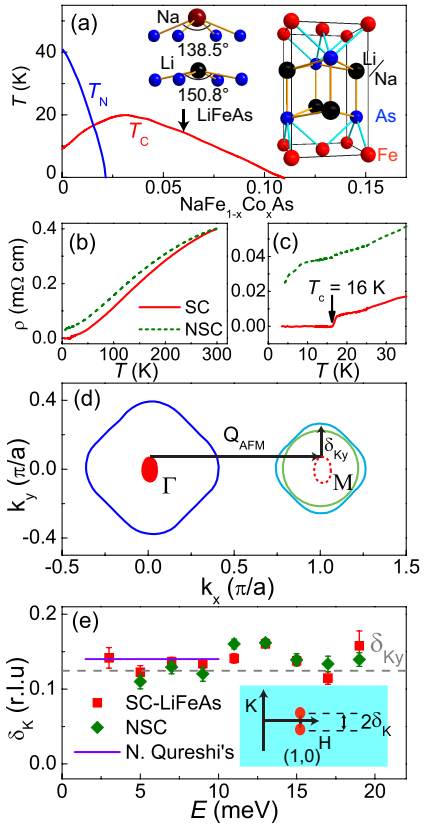

FIG. 1: (color online). (a) Phase diagram of the electron doped $NaFe_{1-x}Co_xAs$ from Ref. [27]. The inset shows the structure of Na(Li)FeAs and the differences in the angles of the two alkali arsenic planes based on the structural parameters from Ref. [8] for LiFeAs and Ref. [26] for NaFeAs. (b) The temperature dependence of resistivity for the SC LiFeAs (solid line) and NSC $Li_{0.94}FeAs$ (dashed line) up to room temperature. The data are normalized by the size and mass of the single crystals. (c) Expanded view of the temperature dependence of the resistivity for the SC and NSC $Li_{1-x}FeAs$. The SC LiFeAs has a clear transition to superconductivity at 16 K. (d) Schematic Fermi surfaces of LiFeAs from Ref. [20]. The red shadow indicates a flat band in the center of the $\Gamma(0,0)$ point. The incommensurability from the ARPES measurements is defined as δ_K, the mismatch of the inner hole Fermi surface and electron Fermi surfaces. (e) The energy dependence of the incommensurability for the incommensurate spin excitations from the SC LiFeAs (the red squared symbols), NSC $Li_{0.94}FeAs$ (the olive diamond symbols), and the APRES measurements (the grey dash line). The violet solid line is the incommensurability value from Ref. [21]. The inset shows the locations of the incommensurate peaks near the in-plane AF wave vector $\mathbf{Q} = (1,0)$ in LiFeAs.

These samples were mounted inside a He exchange gas filled thin aluminum can which was mounted directly to the cold-finger of a closed cycle He refrigerator, where the wave vector Q at $(q_x,\ q_y,\ q_z)$ in Å^{-1} is defined as $(H, K, L) = (q_x a/2\pi, q_y b/2\pi, q_z c/2\pi)$ reciprocal lattice units (rlu) with $a = b = 5.316$ Å, and $c = 6.306$ Å.

In our previous inelastic neutron scattering work on

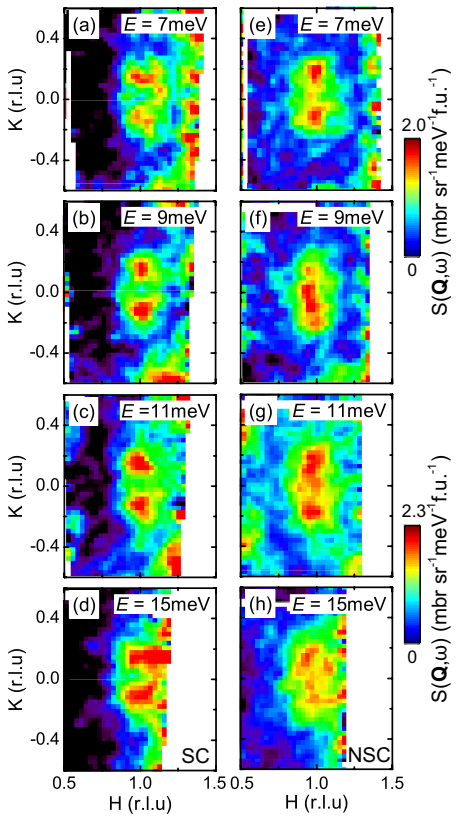

FIG. 2: (color online). Two-dimensional constant-energy plots of the spin excitations in the $[H, K]$ plane at the spin excitation energies indicated (a-d) for the SC LiFeAs and (e-h) for the NSC $Li_{0.94}FeAs$ at 5 K. The incident neutron energy was $E_i = 35$ meV oriented along the c-axis. The intensity has been normalized to be in absolute units using a vanadium standard as discussed in Ref. [25].

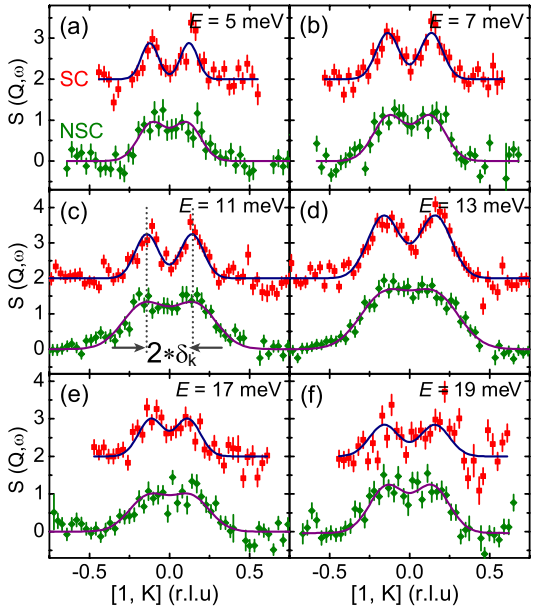

FIG. 3: (color online). Constant-energy cuts of spin excitations along the $[1, K]$ direction for the SC LiFeAs and NSC $Li_{0.94}FeAs$ at energy transfers of (a) $E = 5 \pm 1$ meV; (b) 7 ± 1 meV; (c) 11 ± 1 mV; (d) 13 ± 1 meV; (e) 17 ± 1 meV; (f) 19 ± 1 meV; all with $E_i = 35$ meV. The solid lines are fits to two Gaussian peaks. The dashed vertical lines in (c) marking peak centers, indicate the definition of incommensurability of spin excitations as in previous work [21]. The cuts for the SC and NSC spin excitations spectra were subtracted by the same fitted NSC background at the identical energy. The intensity is in absolute units, and error bars indicate one standard deviation. For presentation, the SC data are offset vertically by 2 units for all panels.

the NSC $Li_{0.94}FeAs$ with natural Li [25], we have reported the presence of a large spin gap of $\Delta = 13$ meV at the AF ordering wave vector $Q = (1, 0, 3)$ using triple-axis spectroscopy. The gap was found to be temperature independent between 2 and 190 K [25]. More recently, inelastic neutron scattering experiments on the SC LiFeAs with the ^{7}Li isotope found low-energy ($1.5 \leq E \leq 13$ meV) transverse incommensurate spin excitations that appear to couple to T_c [21]. In the light of this development, we have carried out new measurements on ARCS with the incident neutron beam direction parallel to the c-axis and $E_i = 35$ meV for both the SC LiFeAs and NSC $Li_{0.94}FeAs$ at 5 K. Figure 2 summarizes the outcome of these measurements. For the SC LiFeAs, Figures 2a-2d show constant-energy (E) images of the scattering in the (H, K) plane for $E = 7 \pm 1$, 9 ± 1, 11 ± 1, and 15 ± 1 meV, respectively. Consistent with previous work [21], we can see clear transverse incommensurate peaks centered near the in-plane AF wave vector $\mathbf{Q} = (1, 0)$ at all the probed energies. Figures 2e-2h plot two-dimensional scattering images for the NSC $Li_{0.94}FeAs$ at $E = 7 \pm 1$, 9 ± 1, 11 ± 1, and 15 ± 1 meV, respectively. These results reveal the presence of low-energy spin excitations in the NSC $Li_{0.94}FeAs$, different from the earlier triple-axis measurement [25]. While spin excitations are clearly incommensurate at the probed energies for the SC LiFeAs (Figs. 2a-2d), the incommensurability is less well-defined for the NSC $Li_{0.94}FeAs$ (Figs. 2e-2h).

To quantitatively determine the differences in spin excitations of the SC and NSC $Li_{1-x}FeAs$, we cut through the transverse direction of the two-dimensional scattering images in Fig. 2. Figures 3a-3f show constant-energy cuts along the $[1, K]$ direction for energies of $E = 5 \pm 1$, 7 ± 1, 11 ± 1, 13 ± 1, 17 ± 1, and 19 ± 1 meV, respectively. Inspection of the Figure reveals that the incommensurabilities of spin excitations for both the SC and NSC $Li_{1-x}FeAs$ are very similar and nearly energy independent for the energy range $5 \leq E \leq 19$ meV. However, the incommensurate spin excitations in the SC LiFeAs have better defined peaks with longer spin-spin correlation lengths compared with that of the NSC $Li_{0.94}FeAs$. Simple Gaussian fits to the data in Fig. 3 are able to extract the incommensurate peak position, δ_K, as a function of energy transfer. This is shown in Fig. 1e, again illustrating the similar

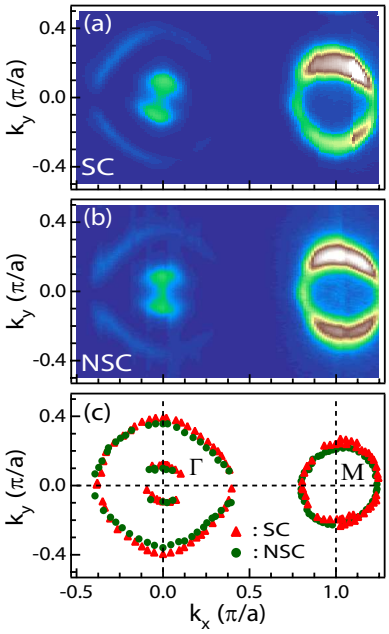

FIG. 4: (color online). (a) and (b) ARPES intensity mappings of the SC and NSC $Li_{1-x}FeAs$ samples recorded with $h\nu = 35$ eV photons (Corresponding to the c-axis momentum transfer $k_Z = \pi$) and integrated within ± 20 meV with respect to the Fermi energy E_F. The extracted Fermi surface contours from (a) and (b) are plotted together in (c).

amount of and the lack of change of incommensurability with energy transfer in both compounds. Based on these data, we see that the low-energy spin excitations in the superconductivity-suppressed $Li_{0.94}FeAs$ are remarkable similar to those of the SC LiFeAs. This implies that the Li-deficiency induced suppression of superconductivity does not fundamentally alter the magnetic properties of the SC LiFeAs.

If we assume that the Li-deficiencies in $Li_{1-x}FeAs$ remove electrons from the FeAs octahedra, the SC LiFeAs should have a larger electron-doping level than that of the NSC $Li_{0.94}FeAs$ and therefore should have a larger electron Fermi surface size. Figures 4a and 4b show the ARPES intensity mappings of the SC LiFeAs and NSC $Li_{0.94}FeAs$, respectively. Figure 4c plots the corresponding hole and electron Fermi pockets near the $\Gamma(0,0)$ and $M(1,0)/(0,1)$ points, respectively, for the SC and NSC samples. To within the errors of our measurements, we find that the SC LiFeAs and NSC $Li_{0.94}FeAs$ have the same Fermi surface topology (Fig. 4c). Therefore, a few percent of Li-deficiencies in $Li_{1-x}FeAs$ does not dramatically change the hole and electron Fermi pocket sizes and alter the Fermi surface nesting conditions. This is consistent with the similar incommensurate spin excitations in the SC and NSC $Li_{1-x}FeAs$ (Figs. 2 and 3), but contrary to the naive expectation that the Li-deficiencies in $Li_{1-x}FeAs$ should reduce the sizes of the electron Fermi surface and enlarge the hole Fermi surface (hole doping).

In previous work, nonmagnetic Zn impurities were found to severely suppress superconductivity for $LaFeAsO_{1-x}F_x$ in the electron-overdoped regime but were much less effective in reducing T_c for the under and optimally electron doped samples [32]. Similarly, Zn impurities were found to be effective in suppressing superconductivity in $BaFe_{2-x}Co_xAs_2$ [33]. This behavior is consistent with the $s^{\pm}$-wave SC state, where the nonmagnetic impurity scattering should rapidly decrease T_c [34]. If we assume that the Li-vacancies in $Li_{1-x}FeAs$ indeed have a limited impact on the size of the electron and hole Fermi surfaces, the rapid suppression of superconductivity by small amount of Li-deficiencies may indicate that superconductivity in the stoichiometric LiFeAs is in the electron-overdoped regime [34]. To see why this may be the case, we consider the lattice structure of LiFeAs as shown in the inset of Fig. 1a. Compared with the AF ordered $Na_{1-\delta}FeAs$ [26], the FeAs octahedron in LiFeAs is much more compressed with an Fe-As distance of $\sim$2.417 Å [8] similar to the Fe-As distance of $\sim$2.42 Å in the electron-overdoped $NaFe_{1-x}Co_xAs$ with $x = 0.2$ [27]. Although we cannot make a direct extrapolation to the LiFeAs electron doping level from this comparison, we note that LiFeAs is close to the electron-overdoped $NaFe_{1-x}Co_xAs$. To understand why small Li-deficiencies can dramatically suppress superconductivity of the stoichiometric LiFeAs while the Na-deficiencies in $Na_{1-\delta}FeAs$ actually promotes superconductivity [35], we note that the Na ions in $Na_{1-\delta}FeAs$ form a buffer layer rather far removed from the FeAs octahedra whereas the Li ions in LiFeAs are almost in the As-layer of the FeAs octahedra [8, 27].

Assuming that the electric conductivity in LiFeAs arises from the hopping of itinerant electrons between the Fe atoms through the As bridge, the Li-vacancies in LiFeAs near the FeAs octahedra can act as impurity centers which scatter off conduction band electrons. If there are also As deficiencies in the NSC $Li_{1-x}FeAs$ [11], they may also act as impurity scattering to suppress superconductivity, whereas Na deficiencies are far removed from the FeAs octahedra and play a role of hole doping. The correction to T_c by the impurity scattering is a universal function of the impurity scattering rate Γ. For the s^{+-}-wave superconductor, it was shown that the SC transition temperature is completely suppressed if the ratio between Γ and the T_c value without impurities is approximately larger than 1 [36]. The value of Γ can be estimated from the resistivity difference $\Delta\rho_i$ between the Li-deficient and stoichiometric $Li_{1-x}FeAs$ via $\Delta\rho_i = m^*\Gamma/e^2n$, where m^* is the effective mass of quasiparticle and n is the electron density per unit cell. From Figure 1c, we see that $\Delta\rho_i$ is about 0.03 mΩ cm. For LiFeAs, the effective mass is $\sim$5 times the bare electron mass [37]. If there are two itinerant electrons per Fe, we find that $\Gamma \approx 2.2T_c$, which is larger than the critical value of Γ that is needed for completely suppressing T_c. This is consistent with the

picture that the out-of-plane Li-vacancies in LiFeAs play the same role as the nonmagnetic Zn impurities in the electron-overdoped $LaFe_{1-y}Zn_yAsO_{1-x}F_x$ [32].

If the stoichiometric LiFeAs is indeed an electron-overdoped superconductor, it should be located away from the AF instability as $NaFe_{1-x}Co_xAs$ near $x \approx 0.065$ (Fig. 1a) without static AF order [26]. The electron doping of $x \approx 0.065$ is roughly estimated from a comparison of incommensurate spin excitations in $BaFe_{2-x}Ni_xAs_2$ [31] with the expected location of incommensurate spin excitations in $NaFe_{1-x}Co_xAs$ [27]. The quasiparticle excitations between the mismatched hole and electron Fermi surfaces due to the self electron-doping should produce incommensurate spin fluctuations along the direction transverse to the AF ordering wave vector $\mathbf{Q} = (1, 0)$ (Figs. 1d and 1e) consistent with the calculated spin susceptibility $\chi''(\mathbf{Q}, \omega)$ based on a random phase approximation of a three-dimensional 5-orbital tight-binding model for $BaFe_2As_2$ [30, 31, 38]. Experimentally, the transverse incommensurate spin fluctuations with $\delta_K \approx 0.1$ were found at $E = 7$ meV for the electron overdoped $BaFe_{2-x}Ni_xAs_2$ at $x = 0.15$ [31]. Using the ARPES measurements (Fig. 4), we plot in Fig. 1d the hole and electron Fermi surfaces of the SC and NSC $Li_{1-x}FeAs$. Assuming that the large hole pocket near $\Gamma(0, 0)$ is unfavorable for the Fermi surface nesting, we see that the nesting of the small hole pocket near $\Gamma(0, 0)$ and the electron pockets near $M(1, 0)/(0, 1)$ should yield incommensurate spin excitations at δ_K as shown in Fig. 1e. This nesting condition is consistent with previous work on LiFeAs [21] and our own measurements. These results are also in agreement with the Fermi surface nesting interpretation of the low-energy spin excitations in the electron- [30, 31] and hole-doped [39, 40] $BaFe_2As_2$, and thus suggest that the stoichiometric LiFeAs is an intrinsically electron-overdoped superconductor. This is also consistent with the fact that further electron-doping in the SC LiFeAs via Ni and Co substition can systematically reduce T_c [11]. We note that for the electron-underdoped $BaFe_{2-x}T_xAs_2$ with static transverse incommensurate spin-density-wave order [22, 23], low-energy (< 10 meV) spin excitations are commensurate [31], and different from the low-energy incommnesurate spin excitations in the SC and NSC $Li_{1-x}FeAs$ (Fig. 2). Therefore, the SC LiFeAs cannot be in the electron-underdoped regime, where Li-deficiencies should have weak effect on superconductivity and further electron-doping should increase T_c.

Moreover, recent systematic scanning tunneling microscopy (STM) measurements on $NaFe_{1-x}Co_xAs$ reveal that the tunneling spectra dI/dV change from the symmetric lineshape around Fermi energy for the optimally electron doped sample ($x = 0.028$) to a strong asymmetric lineshape in the electron overdoped regime ($x = 0.061$) [28]. Since STM measurements on the SC LiFeAs (see Fig. 1b in Ref. [15]) show strong asymmetric tunneling spectra consistent with that of the electron overdoped $NaFe_{1-x}Co_xAs$ with $x = 0.061$ [28], it is inevitable that the SC and NSC $Li_{1-x}FeAs$ are in the electron overdoped regime similar to the electron overdoped $NaFe_{1-x}Co_xAs$ (Fig. 1a). This is also consistent with the fact that superfluid density in LiFeAs lies away from the Uemura plot for regular FeAs, but behaves more like an electron overdoped cuprates [9, 41].

CONCLUSIONS

In summary, we have shown that the stoichiometric LiFeAs is an electron overdoped superconductor. Moreover, we find that small Li-deficiencies in $Li_{1-x}FeAs$ suppress superconducitivity via an impurity scattering effect. Therefore, in spite of the absent static AF order and the shallow hole Fermi pockets near the $\Gamma(0, 0)$ point [13], the fundamental SC mechanism in LiFeAs is similar to all other iron-based superconductors.

ACKNOWLEDGMENTS

We thank P. Richard, T. Qian, Zhuan Xu, Shiliang Li, and Yayu Wang for helpful discussions. The work in IOP is supported by the MOST of China through 973 projects: 2012CB821400, 2010CB833102, and 1J2010CB923001. The work at UTK is supported by the U.S. DOE BES No. DE-FG02-05ER46202. The research at ORNL's SNS was sponsored by the Scientific User Facilities Division, BES, U.S. DOE. The ARPES work at SRC is primarily funded by the University of Wisconsin-Madison with supplemental support from facility Users and the University of Wisconsin-Milwaukee.

* Electronic address: pdai@utk.edu

[1] Y. Kamihara, T. Watanabe, M. Hirano, and H. Hosono, J. Am. Chem. Soc. **130**, 3296 (2008).
[2] C. de la Cruz, Q. Huang, J. W. Lynn, J. Li, W. Ratcliff II, J. L. Zarestky, H. A. Mook, G. F. Chen, J. L. Luo, N. L. Wang, and P. C. Dai, Nature (London) **453**, 899 (2008).
[3] M. D. Lumsden and A. D. Christianson, Magnetism in Fe-based superconductors. J. Phys.: Condens. Matter **22**, 203203 (2010).
[4] J. W. Lynn and P. C. Dai, Physica C **469**, 469 (2009).
[5] P. C. Dai, J. P. Hu, and E. Dagotto, arXiv:1209.0381 (Nat. Phys., in the press).
[6] X. C. Wang, Q. Q. Liu, Y.X. Lv, W.B. Gao, L. X. Yang, R. C. Yu, F. Y. Li, C. Q. Jin, Solid State Commun. **148** , 538 (2008).
[7] J. H. Tapp, Z. Tang, B. Lv, K. Sasmal, B. Lorenz, P. C.W. Chu, and A. M. Guloy, Phys. Rev. B **78**, 060505(R) (2008).

[8] M. J. Pitcher, D. R. Parker, P. Adamson, S. J. C. Herkelrath, A. T. Boothroyd, R. M. Ibberson, M. Brunelli, and S. J. Clarke, Chem. Commun., 5918 (2008).

[9] F. L. Pratt, P. J. Baker, S. J. Blundell, T. Lancaster, H. J. Lewtas, P. Adamson, M. J. Pitcher, D. R. Parker, and S. J. Clarke, Phys. Rev. B **79**, 052508 (2009).

[10] C. W. Chu, F. Chen, M. Gooch, A.M. Guloy, B. Lorenz, B. Lv, K. Sasmal, Z. J. Tang, J. H. Tapp, Y. Y. Xue, Physica C **469**, 326 (2009).

[11] M. J. Pitcher, T. Lancaster, J. D. Wright, I. Franke, A. J. Steele, P. J. Baker, F. L. Pratt, W. T. Thomas, D. R. Parker, S. J. Blundell, and S. J. Clarke. J. Am. Chem. Soc. **132**, 10467 (2010).

[12] D. J. Scalapino, arXiv: 1207.4093 (Rev. Mod. Phys., in press).

[13] S. V. Borisenko, V. B. Zabolotnyy, D. V. Evtushinsky, T. K. Kim, I. V. Morozov, A. N. Yaresko, A. A. Kordyuk, G. Behr, A. Vasiliev, R. Follath, and B. Büchner, Phy. Rev. Lett. **105**, 067002 (2010).

[14] P. M. R. Brydon, M. Daghofer, C. Timm, and J. van den Brink, Phys. Rev. B **83**, 060501(R) (2011).

[15] T. Hänke, S. Sykora, R. Schlegel, D. Baumann, L. Harnagea, S. Wurmehl, M. Daghofer, B. Büchner, J. van den Brink, and C. Hess, Phys. Rev. Lett. **108**, 127001 (2012).

[16] P. J. Hirschfeld, M. M. Korshunov, I. I. Mazin, Rep. Prog. Phys. **74**, 124508 (2011).

[17] K. Kuroki, S. Onari, R. Arita, H. Usui, Y. Tanaka, H. Kontani, and H. Aoki, Phys. Rev. Lett. **101**, 087004 (2008).

[18] A. V. Chubukov, Annu. Rev. Condens. Matter Phys. **3**, 13 (2012).

[19] F. Wang, Hui Zhai, Y. Ran, A. Vishwanath, and D.-H. Lee, Phys. Rev. Lett. **102**, 047005 (2009).

[20] K. Umezawa, Y. Li, H. Miao, K. Nakayama, Z.-H. Liu, P. Richard, T. Sato, J. B. He, D.-M. Wang, G. F. Chen, H. Ding, T. Takahashi, and S.-C. Wang, Phys. Rev. Lett. **108**, 037002 (2012).

[21] N. Qureshi, P. Steffens, Y. Drees, A. C. Komarek, D. Lamago, Y. Sidis, L. Harnagea, H.-J. Grafe, S. Wurmehl, B. Büchner, and M. Braden, Phys. Rev. Lett. **108**, 117001 (2012).

[22] D. K. Pratt, M. G. Kim, A. Kreyssig, Y. B. Lee, G. S. Tucker, A. Thaler, W. Tian, J. L. Zarestky, S. L. Bud'ko, P. C. Canfield, B. N. Harmon, A. I. Goldman, and R. J. McQueeney. Phys. Rev. Lett. **106**, 257001 (2011).

[23] H. Q. Luo, R. Zhang, M. Laver, Z. Yamani, M. Wang, X. Y. Lu, M. Y. Wang, Y. C. Chen, S. Li, S. Chang, J. W. Lynn, and P. C. Dai, Phys. Rev. Lett. **108**, 247002 (2012).

[24] A. E. Taylor, M. J. Pitcher, R. A. Ewings, T. G. Perring, S. J. Clarke, and A. T. Boothroyd, Phys. Rev. B **83**, 220514 (R) (2011).

[25] M. Wang, X. C. Wang, D. L. Abernathy, L. W. Harriger, H. Q. Luo, Y. Zhao, J. W. Lynn, Q. Q. Liu, C. Q. Jin, C. Fang, J. P. Hu, and Pengcheng Dai, Phys. Rev. B **83**, 220515 (R) (2011).

[26] S. L. Li, C. de la Cruz, Q. Huang, G. F. Chen, T.-L. Xia, J. L. Luo, N. L. Wang, and P. C. Dai, Phys. Rev. B **80**, 020504(R) (2009).

[27] D. R. Parker, M. J. P. Smith, T. Lancaster, A. J. Steele, I. Franke, P. J. Baker, F. L. Pratt, M. J. Pitcher, S. J. Blundell, and S. J. Clarke, Phys. Rev. Lett. **104**, 057007 (2010).

[28] X. D. Zhou, P. Cai, A. F. Wang, W. Ruan, C. Ye, X. H. Chen, Y. Z. You, Z.-Y. Weng, and Y. Y. Wang, Phys. Rev. Lett. **109**, 037002 (2012).

[29] C. Lester, J.-H. Chu, J. G. Analytis, T. G. Perring, I. R. Fisher, and S. M. Hayden, Phys. Rev. B **81**, 064505 (2010).

[30] J. T. Park, D. S. Inosov, A. Yaresko, S. Graser, D. L. Sun, Ph. Bourges, Y. Sidis, Yuan Li, J.-H. Kim, D. Haug, A. Ivanov, K. Hradil, A. Schneidewind, P. Link, E. Faulhaber, I. Glavatskyy, C. T. Lin, B. Keimer, and V. Hinkov, Phys. Rev. B **82**, 134503 (2010).

[31] H. Q. Luo, Z. Yamani, Y. C. Chen, X. Y. Lu, M. Wang, S. L. Li, T. A. Maier, S. Danilkin, D. T. Adroja, and P. C. Dai, Phys. Rev. B **86**, 024508 (2012).

[32] Y. K. Li, J. Tong, Q. Tao, C. M. Feng, G. H. Cao, W. Q. Chen, F. C. Zhang and Z.-A. Xu, New J. Phys. **12**, 083008 (2010).

[33] J. Li, Y. F. Guo, S. B. Zhang, Y. Tsujimoto, X. Wang, C.I. Sathish, S. Yu, K. Yamaura, E. Takayama-Muromachi, Solid State Communications **152**, 671 (2012).

[34] R. M. Fernandes, M. G. Vavilov, and A. V. Chubukov, Phys. Rev. B **85**, 140512 (R) (2012).

[35] M. A. Tanatar, N. Spyrison, K. Cho, E. C. Blomberg, G. T. Tan, P. C. Dai, C. L. Zhang, and R. Prozorov, Phys. Rev. B **85**, 014510 (2012).

[36] Y. Bang, H. Y. Choi, H. Won, Phys. Rev. B **79**, 054529 (2009).

[37] C. Putzke, A. I. Coldea, I. Guillamón, D. Vignolles, A. McCollam, D. LeBoeuf, M. D. Watson, I. I. Mazin, S. Kasahara, T. Terashima, T. Shibauchi, Y. Matsuda, and A. Carrington, Phys. Rev. Lett. **108**, 047002 (2012).

[38] S. Graser, A. F. Kemper, T. A. Maier, H.-P. Cheng, P. J. Hirschfeld, and D. J. Scalapino, Phys. Rev. B **81**, 214503 (2010).

[39] C. L. Zhang, M. Wang, H. Q. Luo, M. Y. Wang, M. S. Liu, J. Zhao, D. L. Abernathy, T. A. Maier, Karol Marty, M. D. Lumsden, S. X. Chi, S. Chang, J. A. Rodriguez-Rivera, J. W. Lynn, T. Xiang, J. P. Hu, and P. C. Dai, Scienific Reports **1**, 115 (2011).

[40] J.-P. Castellan, S. Rosenkranz, E. A. Goremychkin, D. Y. Chung, I. S. Todorov, M. G. Kanatzidis, I. Eremin, J. Knolle, A. V. Chubukov, S. Maiti, M. R. Norman, F. Weber, H. Claus, T. Guidi, R. I. Bewley, and R. Osborn, Phys. Rev. Lett. **107**, 177003 (2011).

[41] T. Goko, A. A. Aczel, E. Baggio-Saitovitch, S. L. Budko, P. C. Canfield, J. P. Carlo, G. F. Chen, P. Dai, A. C. Hamann, W. Z. Hu, H. Kageyama, G. M. Luke, J. L. Luo, B. Nachumi, N. Ni, D. Reznik, D. R. Sanchez-Candela, A. T. Savici, K. J. Sikes, N. L. Wang, C. R. Wiebe, T. J. Williams, T. Yamamoto, W. Yu, and Y. J. Uemura, Phys. Rev. B **80**, 024508 (2009).